Influence of changing magnetic field on solar wind outflow

Bala Poduval
Space Science Institute, Boulder, CO

Continuation of Paper I

- Overview
- Summary of Paper I
- New results

Space Weather

changing conditions in the interplanetary medium (solar wind) causing disruptions to technological systems on Earth and nearby space

Solar Wind Origin

solar wind speed α 1/fte

$$fte = \left(\frac{R_{phot}}{R_{ss}}\right)^2 \frac{B_{r(phot)}}{B_{r(ss)}}$$

fte – flux tube expansion factor – between photosphere and source surface;

R_{phot}; R_{ss} – radii of photosphere & source surface

$B_{r(phot)}$; $B_{r(ss)}$ – magnetic field

Wang-Sheeley-Arge Model

WSA: Arge and Pizzo, JGR, 105, 2000

$$v = 265.0 + (1.5/(1+f_s)^{1/2.5}) * (5.8 - 4.0 * \exp(\vartheta_b 2.5)^2))^3$$

(from McGregor et al., JGR, 113, 2008)

f_s - flux expansion factor

ϑ_b - the angular distance of the magnetic field foot point from the nearest coronal hole boundary

WSA/ENLIL

ENLIL: state-of-the-art space weather prediction model of NOAA - Space Weather Prediction Center

WSA provides ambient solar wind at the inner boundary of ENLIL

1 - 4 day advance warnings of geomagnetic storms caused by earth-directed CMEs & quasi-recurrent solar wind structures

error: 1-2 days

major single source: WSA background solar wind, due to intrinsic flaws in PFSS model (e.g. Pizzo et al., Space weather, 2012) reduce error & improve inner boundary conditions of ENLIL

PAPER 1

- ApJ L, **782**, L22:
- Model: CSSS (compared with PFSS)
- SWS—FTE: quadratic equation for Wand & Sheeley relation
- Data: WSO & NSO/Kitt Peak — 1996-1998 (CRs1910-1945)
- Metric of accuracy: RMSE between predicted & observed SWS

Paper 1

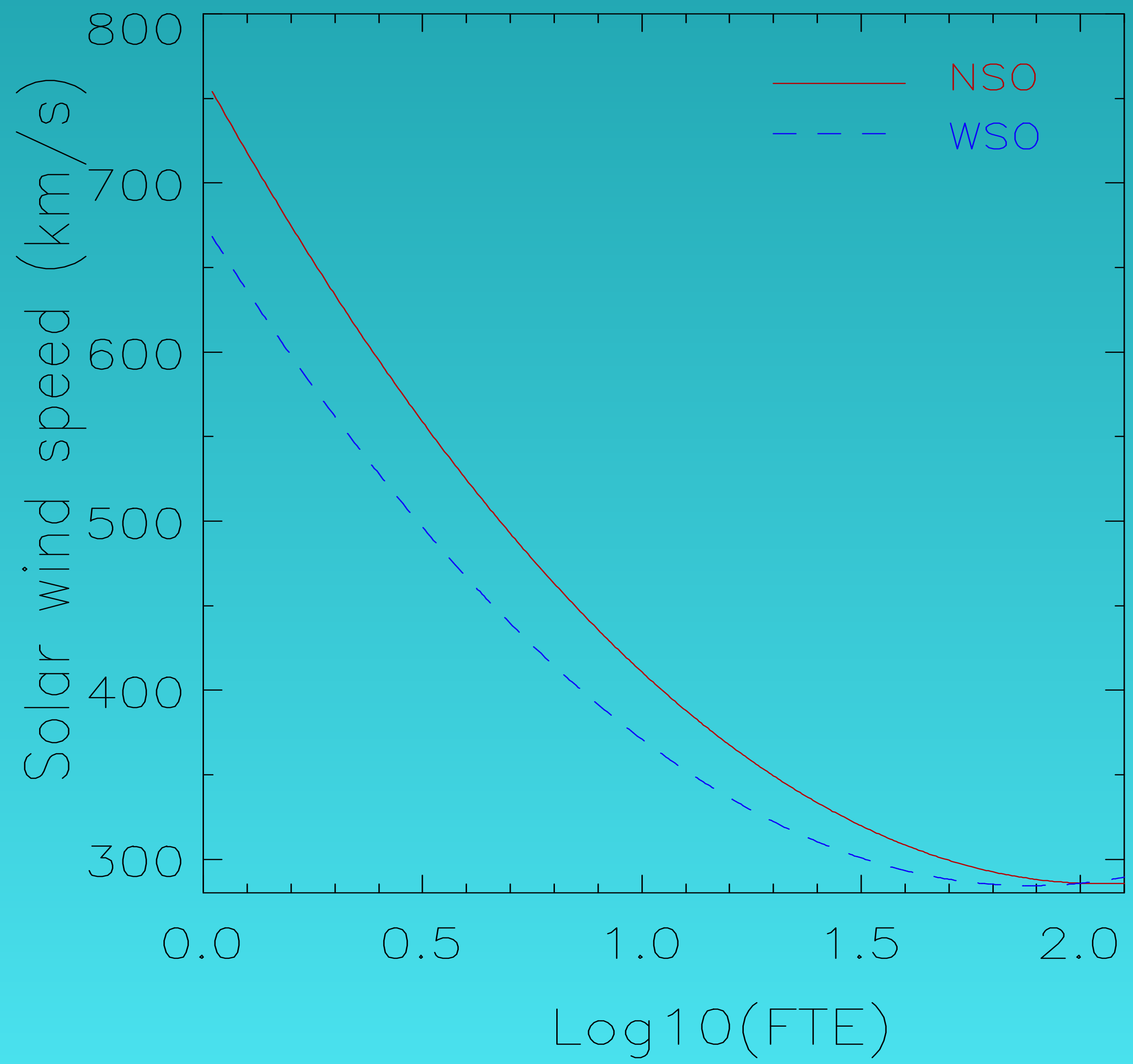

WSO

a = 110.3

b = -416.0

c = 676.6

NSO/Kitt Peak

a = 113.9

b = 466.6

c = 763.4

Paper 1

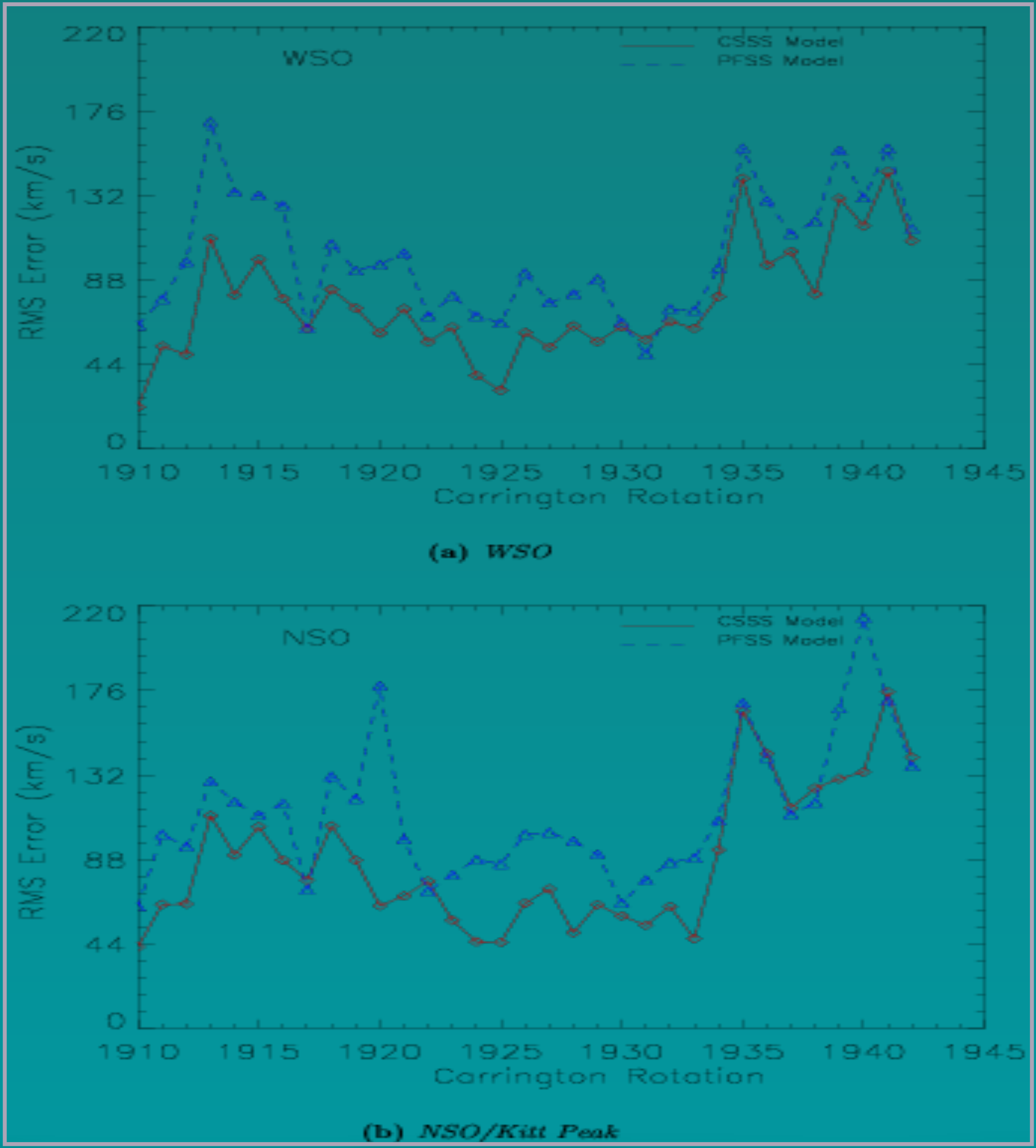

(a) *WSO*

(b) *NSO/Kitt Peak*

RMSE increases as solar cycle progresses —> (1) difficulty modelling complex magnetic field. (2) Optimization of free parameters:

R_{SS} = 15 Rsun or closer?

Rcp = 2.5 Rsun?

Height of cusp varies over wide range (see e.g. Cranmer et al., 2007 Zhao & Hoeksema, 1995)

PAPER I

		WSO	NSO	
cor coft > 0.5	CSSS	24%	24%	
	PFSS	15%	15%	
mean cor coft	CSSS	0.15	0.23	
	PFSS	0.12	0.13	
Mean RMSE ratio	WSA-ENLIL/CSSS	-	-	1.9
Mean RMSE ratio	pfss/csss	1.3	1.6	
RMSE > 1.3:		32%	55%	

82% with RMSE >= 1.0 —> CSSS predictions are comparable to or better than PFSS predictions

Paper 1

PFSS: magnetic field constrained to be radial at 2.5 Rsun

—>larger uncertainties in the photospheric foot points

CSSS: magnetic fields allowed to be nonradial

between 2.5 R_{sun} and 15 R_{sun}

Better performance of CSSS model indicates solar wind sources are traced more accurately — nearly twice better than PFSS & WSA/ENLIL

PFSS Model

popular – addresses a variety of solar/coronal problems

CSSS Model

BOGDAN & LOW 1986 obtained solution to magnetostatic equilibrium — electric currents flowing perpendicular to gravity ($1/r^2$) everywhere

$$J = \frac{1}{\mu_0 r}[1-\eta(r)]\left[\frac{1}{sin(\theta)}\frac{\partial^2\phi}{\partial\phi\partial r}\hat{\phi} - \frac{\partial^2\phi}{\partial\theta\partial r}\hat{\phi}\right] \tag{1}$$

and

$$B = -\eta(r)\frac{\partial\phi}{\partial r}\hat{r} - \frac{1}{r}\frac{\partial\phi}{\partial\theta}\hat{\theta} - \frac{1}{sin(\theta)}\frac{\partial\phi}{\partial\phi}\hat{\phi} \tag{2}$$

where, μ_0 is the magnetic permeability, $\eta(r) = 1 + (a/r)^2$ and $\phi(r, \theta, \phi)$ is a scalar function determined by the boundary conditions at the photosphere and corona (Zhao and Hoeksema, 1995).

CSSS Model - Geometry

inner region

$$\Phi = \sum_{n=1}^{N_\odot} \sum_{m=0}^{n} R_n^\odot(r) P_n^m(\cos\theta)(g_{nm}^\odot \cos m\phi + h_{nm}^\odot \sin m\phi) \qquad (3)$$

$$R_n^\odot(r) = \frac{R_\odot(1+a)^n}{(n+1)(r+a)^{n+1}} \qquad (4)$$

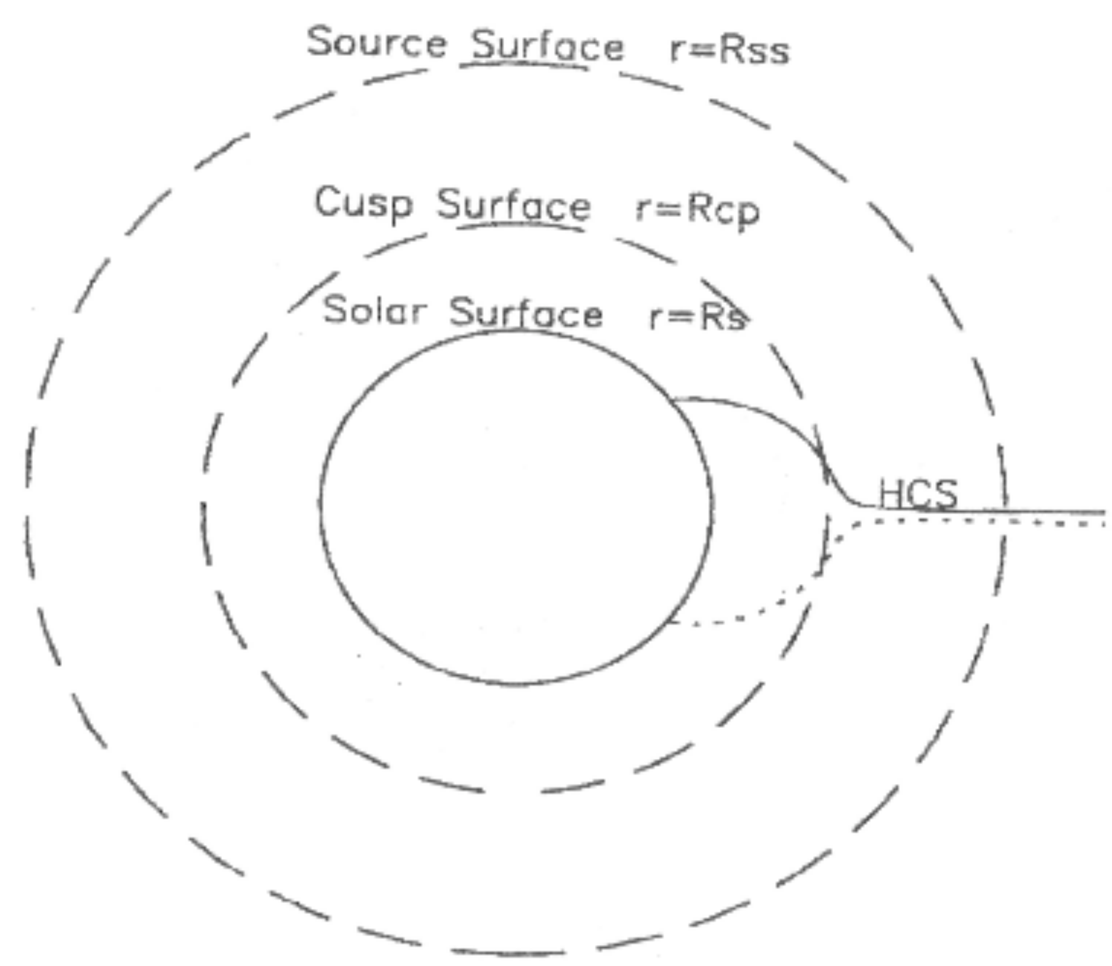

middle region

$$\Phi = \sum_{n=0}^{N_c} \sum_{m=0}^{n} R_n^c(r) P_n^m(\cos\theta)(g_{nm}^c \cos m\phi + h_{nm}^c \sin m\phi)$$

outer region: extrapolate computed B out into the heliosphere

$$B_\theta(R_{ss}, \theta_{ss}, \phi_{ss}) = B_\phi(R_{ss}, \theta_{ss}, \phi_{ss}) = 0$$

DATA

solar cycle 23— early solar cycle 24

OMNI data – Daily averaged solar wind speed 1996-2010

Photospheric synoptic maps:

MDI: (360x180) — 1° (lat, long) resolution

MWO: (91x34); WSO: (72, 30); SOLIS: (360x180)

(CR1900) (CR2006)

No MDI data available outside of this period

Method: Step 1

Step 1: map observed solar wind back to corona

$$\varphi_0 = \varphi_R + \frac{R\Omega}{V_R} \quad \& \quad \vartheta_0 = \vartheta_R$$

ϑ_0, φ_0 – latitude & longitude at source surface

ϑ_R, φ_R – at a distance R from Sun

Ω – angular rotation of the Sun

V_R – the solar wind velocity at R – we used the daily averaged value

Method: Steps 2-4

Step 2: map coronal location back to photosphere along open field lines using CSSS & PFSS models

Step 3: compute FTE at each solar wind source

Step 4: predicted solar wind speed using WS relationship

Speed	FTE
> 750	< 4.5
650 - 750	4.5 - 8
550 - 650	8 - 10
450 - 550	10 - 20
< 450	> 20

RMSE

Evaluate performances of PFSS and CSSS models

Root Mean Square Error (RMSE)
between observed and predicted speeds

$$\text{RMSE ratio} \approx \text{RMSE}_{\text{PFSS}}/\text{RMSE}_{\text{CSSS}}$$

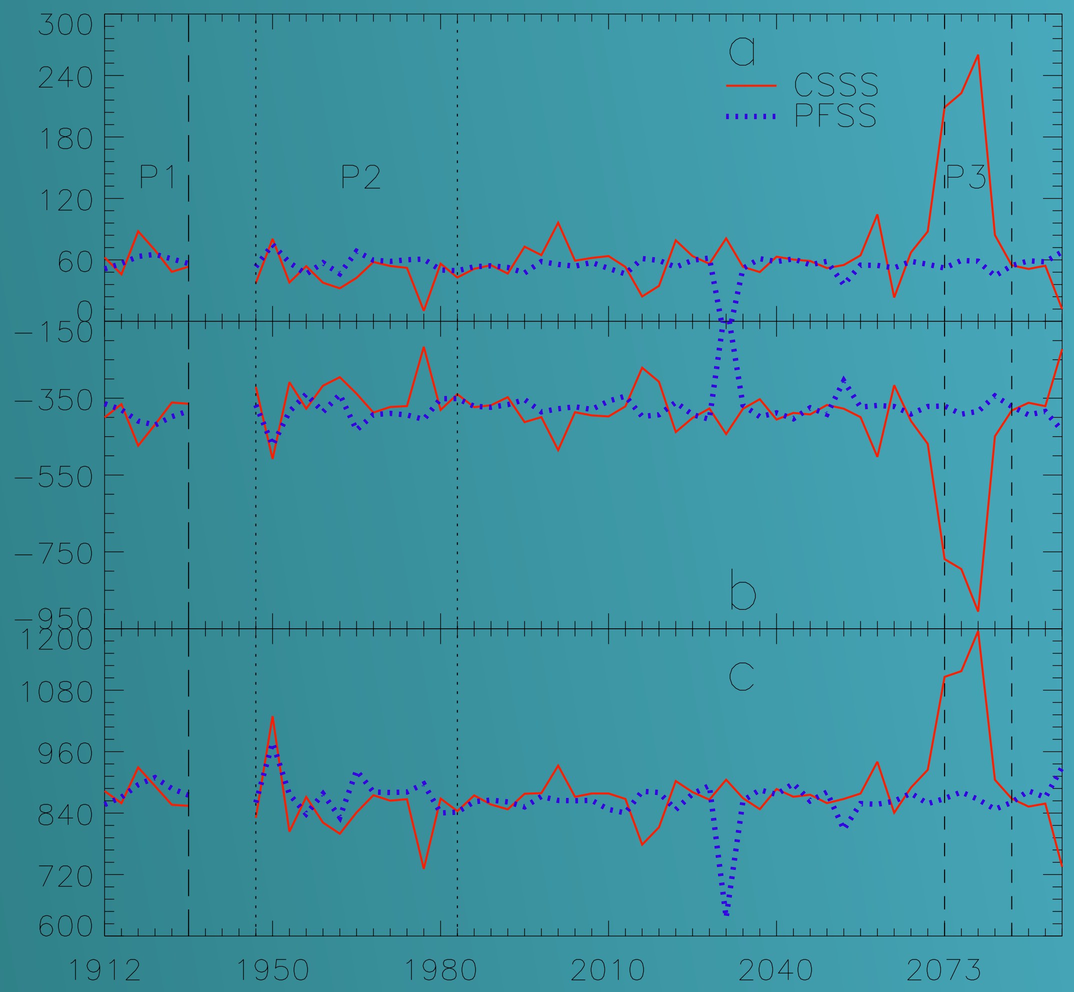

(a) CRs 1912–2104 (1996–2010)

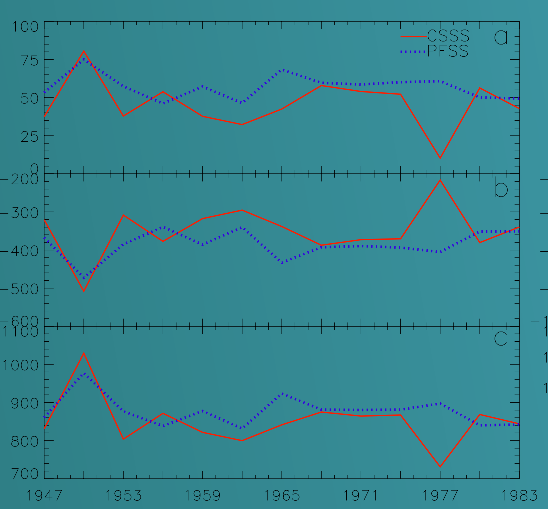

(b) CRs 1947–1985 (1999–2002)

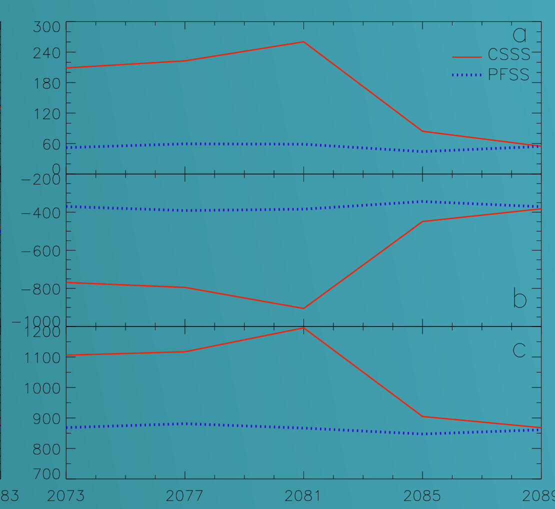

(c) CRs 2073–2092 (2008–2010)

(L) MDI

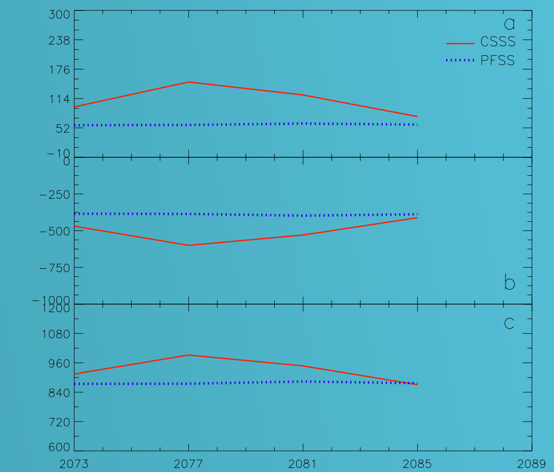

(d) MWO (missing CRs2089–2092)

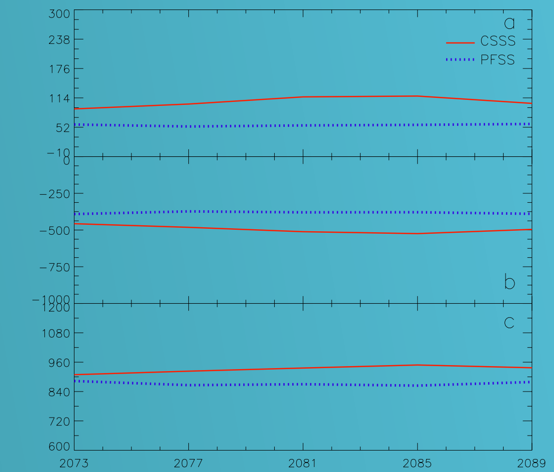

(e) WSO

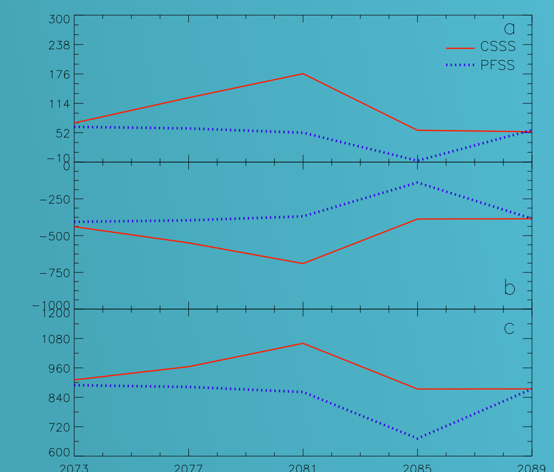

(f) SOLIS (missing CRs2090–2091)

(R) MWO, WSO & SOLIS

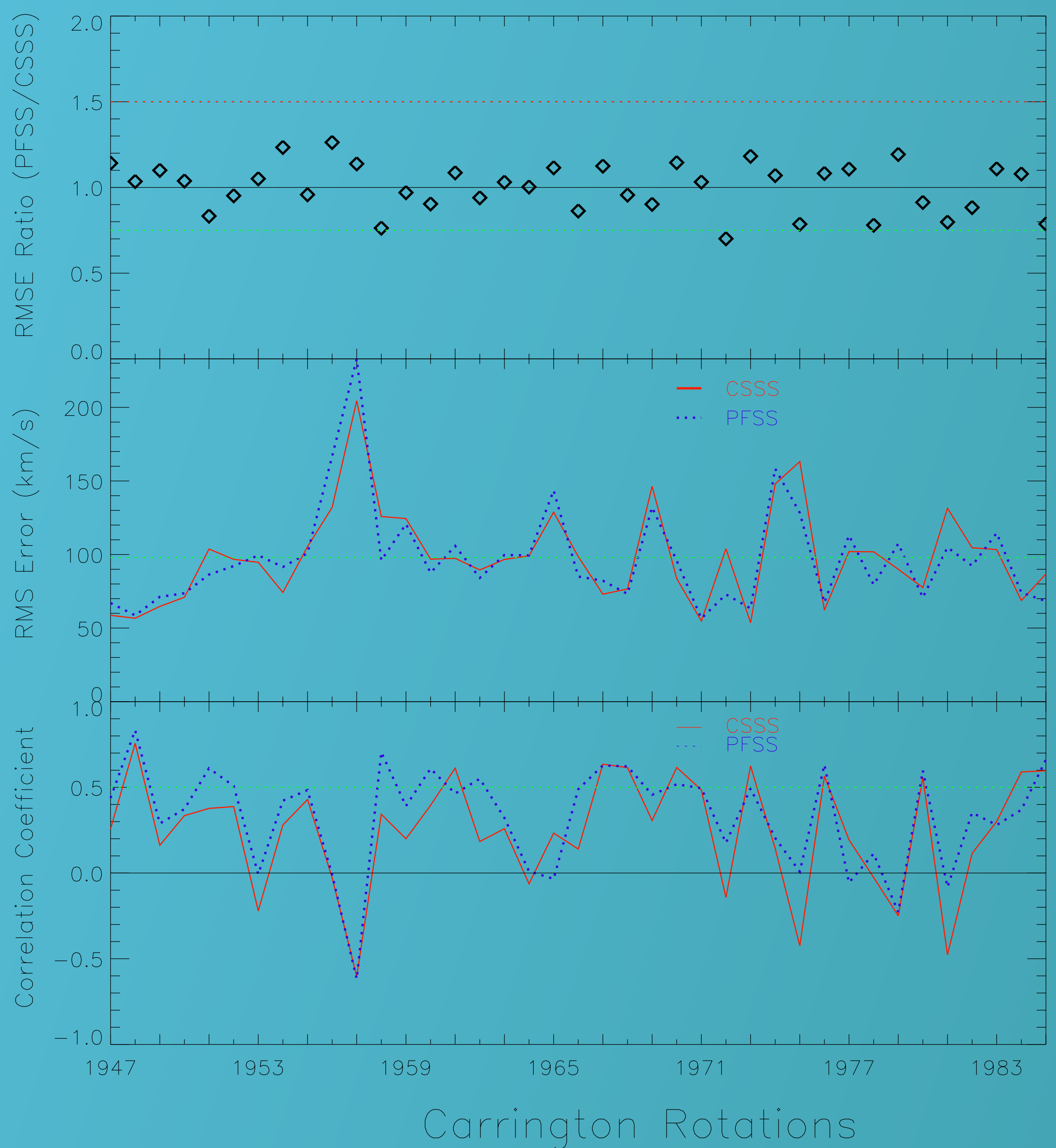

(a) *CRs 1947–1985 (1999–2002).*

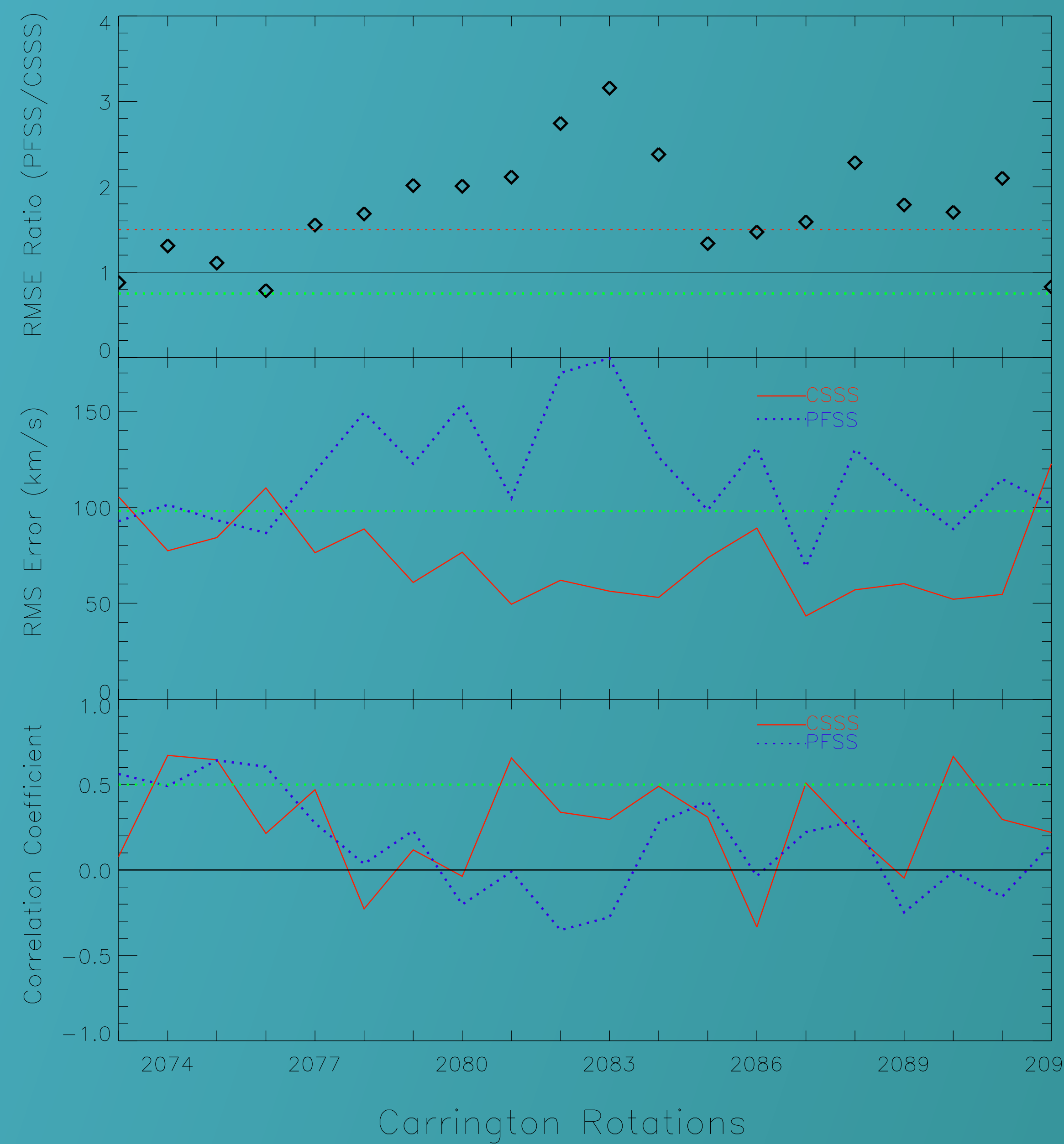

(b) *CRs 2073–2092 (2008–2010).*

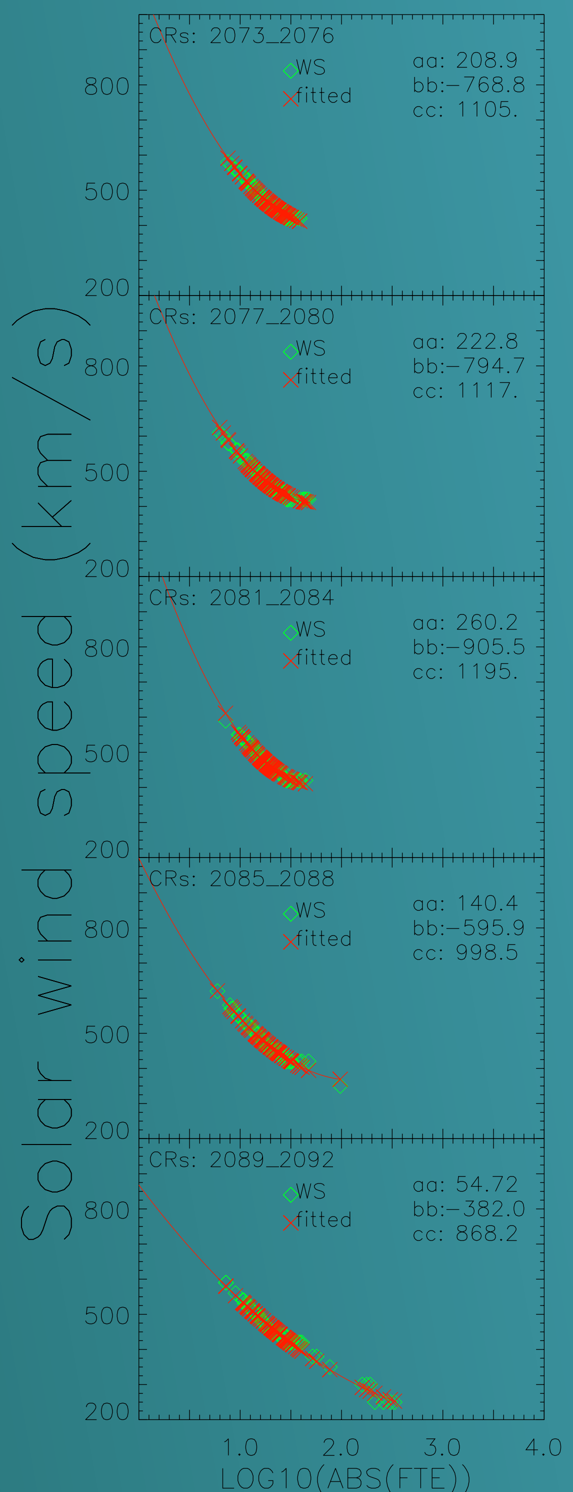

(a) CRs 2073–2092 (2008–2010).

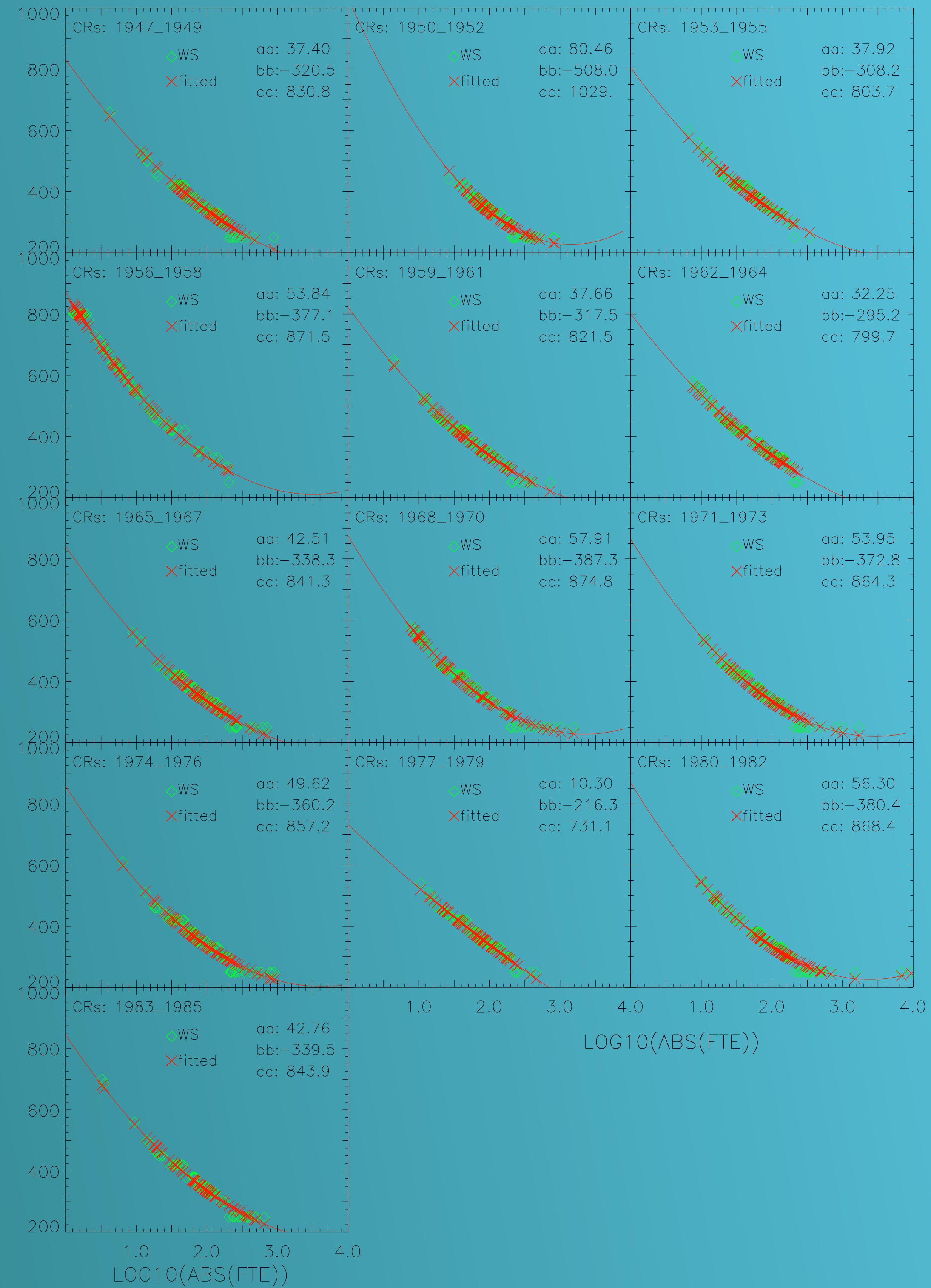

(b) CRs 1947–1985 (1999–2002).

Predicted Solar Wind

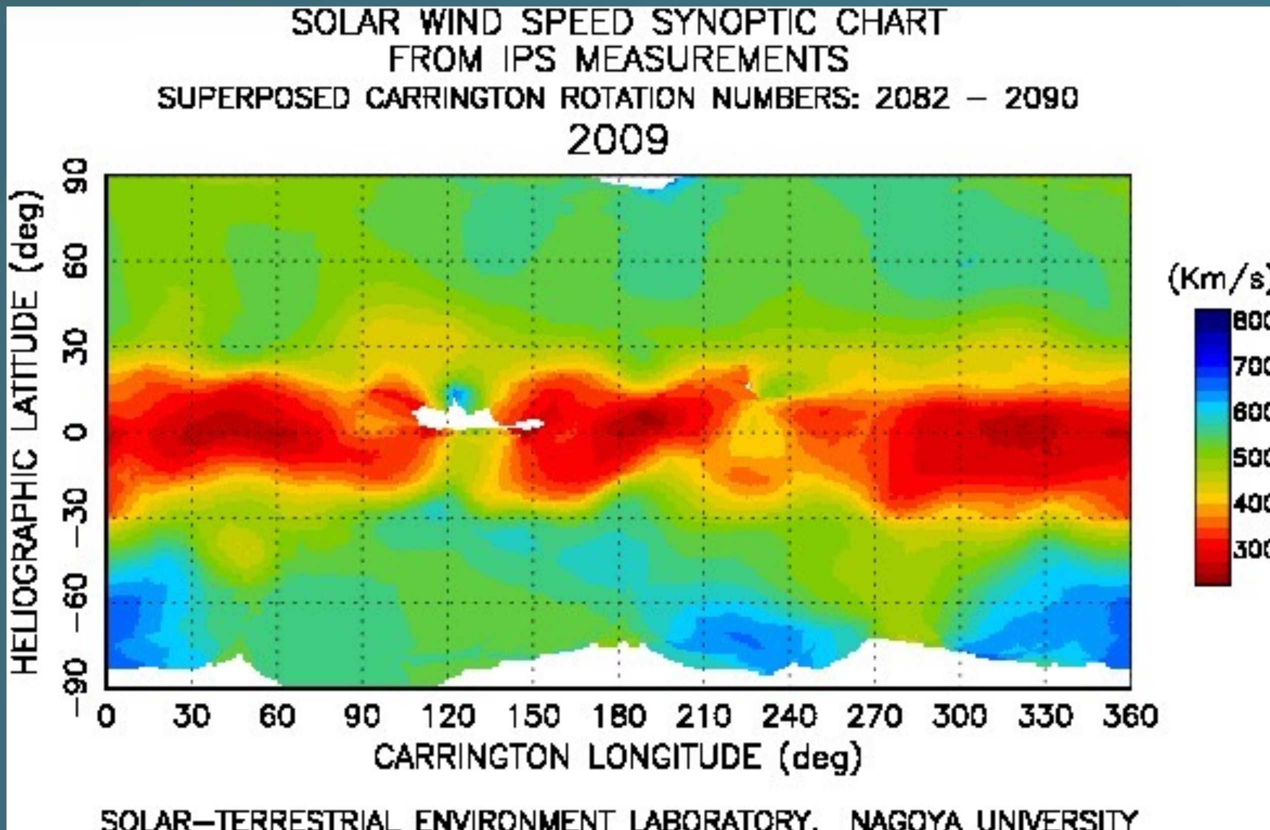

pink: 430km/s blue: 460

light blue: 510green: 560

CR2076 yellow: 610

orange: 640 red: > 700

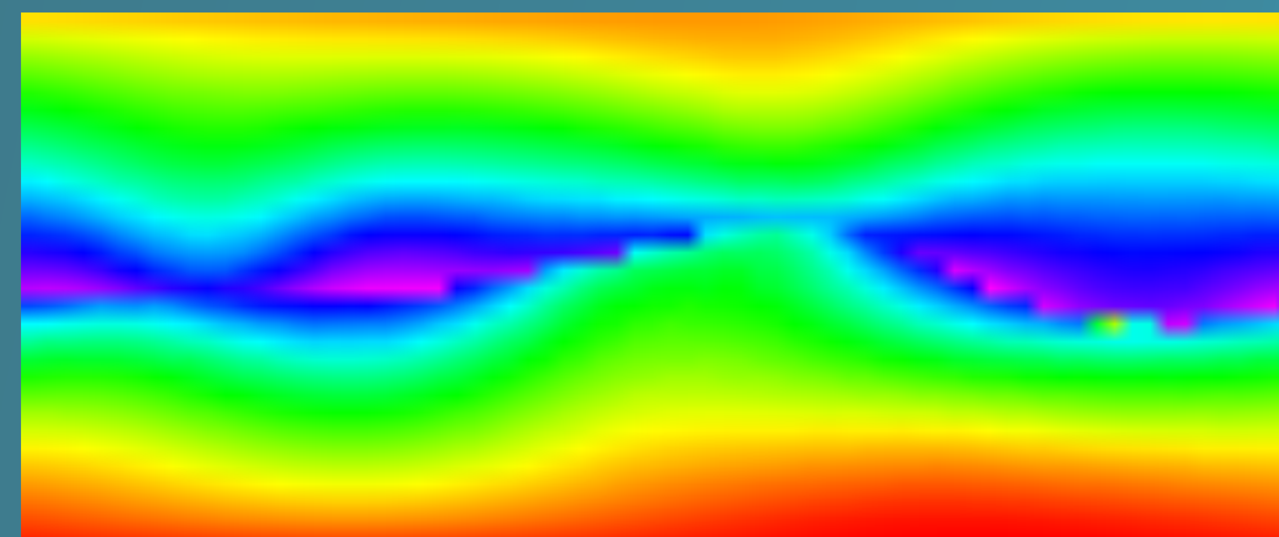

pink: 440km/s blue: 460

light blue: 520

2084 green: 570

yellow: 610

orange: 640 red: > 700

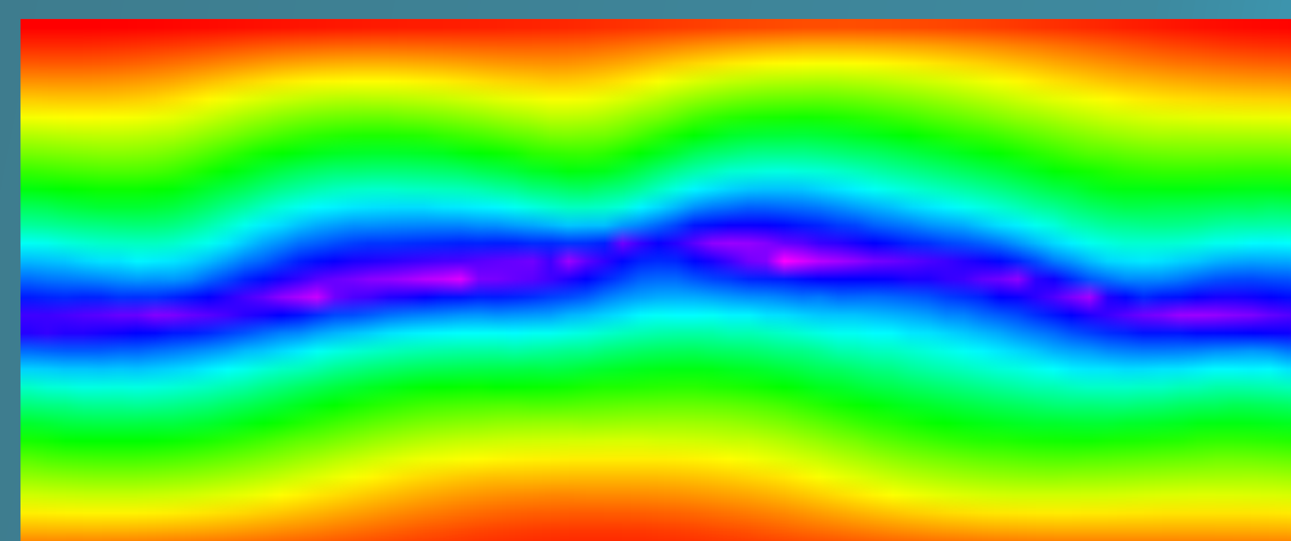

Why the Anomaly?

- log(FTE): 0.8 and 2.3 (Phase~P3)
  0.1 and 4.0 (Phase P2)

- lower value during Phase~P3 —> SWS above 650~km/s not predicted accurately

- high values (> 950~km/s) of the y—intercept (c) support this; seldom occurred in Phase~P2

Why the Anomaly?

- it is well known that the measured polar field strength influences the modulation of the neutral line and thereby the predicted solar wind speed.

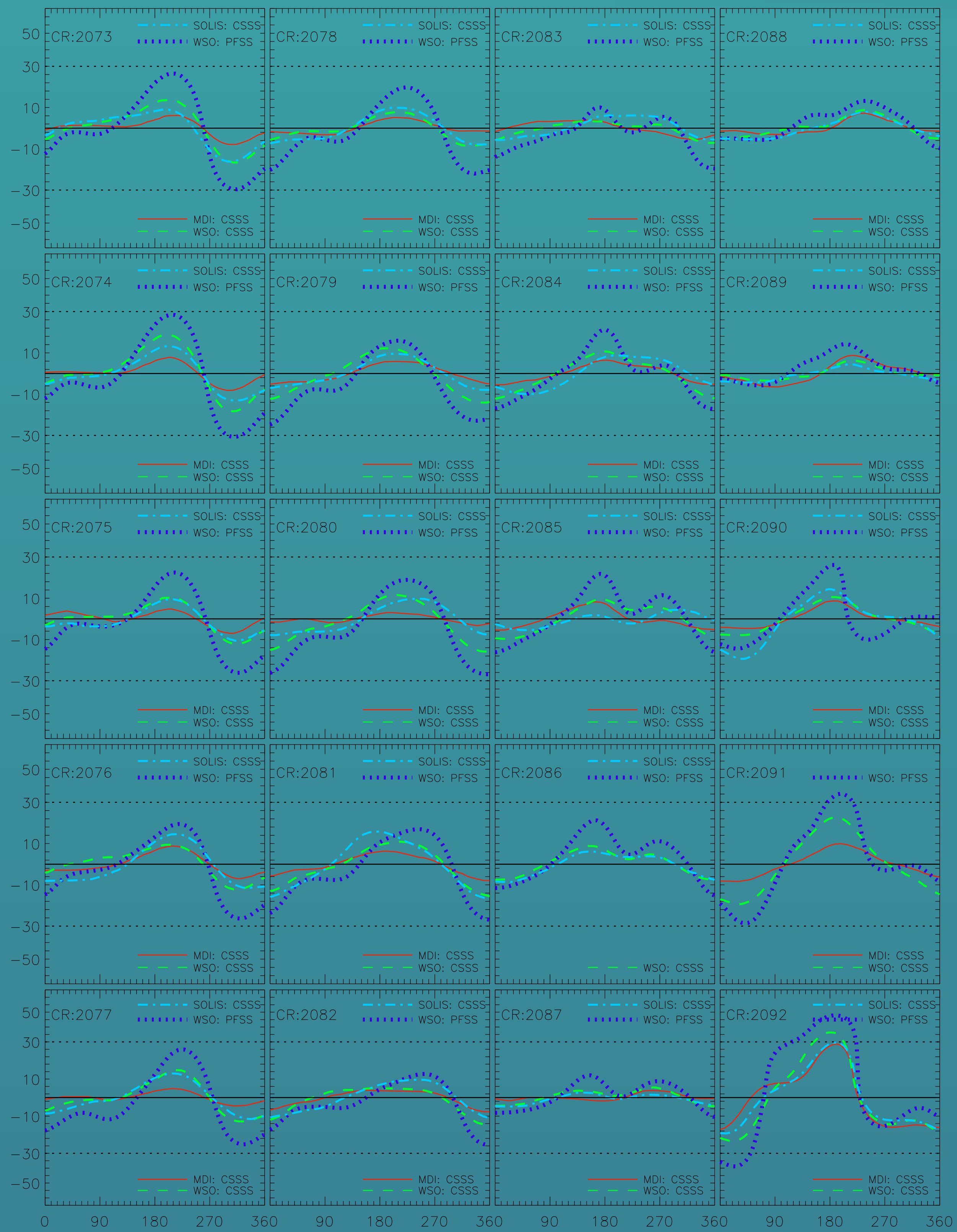

WHY THE ANOMALY?

- Wang et al., (2009): stronger polar fields ⟶ larger polar coronal holes, disappearance/shrinking of low--latitude coronal holes, and flatter HCS
:an increase in the polar coronal hole ⟶ smaller expansion factors (FTE) ⟶ an increase in the polar solar wind speed.

- Gibson et al. (2009): during 2008 there existed numerous low-latitude coronal holes giving rise to frequent high--speed solar wind in the ecliptic.

Why the Anomaly?

- The average unsigned polar field strength:

  MDI MWO SOLIS WSO synoptic maps

  3.6 5.1 4.1 3.8 G during Phase P3.

- These are about 33--45% less than corresponding values around minimum of solar cycle 23 (CRs1911--1931: SOLIS data not available)

WHY THE ANOMALY?

- polar field strengths during 2008--2010 are significantly lower than those of past minima → the argument of Wang et. al., 2009 explains the missing lower values & the temporal variations of the coefficients.

- values between 1.3 and 2.0 are sufficient to predict most of the observed slow wind, the narrow range of log(FTE) during Phase P3 questions the source of solar wind during this period:
small, low--latitude coronal holes and/or pseudostreamers, rather than polar coronal holes — typical solar minimum source of solar wind

CONCLUSIONS

-solar cycle variation - quadratic term in the best fit to speed-FTE

-nearly disappearing during certain solar rotations,

- giving rise to an almost linear fit -

-this variation is significant in CSSS model

-nearly negligible in PFSS model

CONCLUSIONS

- We notice an anomaly in the temporal variations of the coefficients of the fitted quadratic equation during the extended minimum 2008—2010 for CSSS model
- particularly significant when MDI synoptic maps are used
- Similar, but less dramatic, variations shown by other synoptic maps confirm — caused by characteristics of magnetic field during 2008-early 2010 (solar cycle 24).

Conclusions

controlling influence of magnetic field on solar wind outflow

$$FTE = Br(pho)/Br(ss) * (R/Rss)^2$$

Br(pho); R: photospheric magnetic field & radius

Br(ss), Rss: source surface magnetic field & radius

Conclusions

The CSSS model is sensitive to subtle characteristics of the solar magnetic field which in turn is reflected in its better predictive capability during all phases of a solar cycle.

Comparison of Models

PFSS	CSSS
source surface – 2.5 Rsun	Free to vary: 14 - 15 Rsun
magnetic field at SS: open & constrained to be radial	Open at cusp surface 2.5 Rsun but not radial until SS
Coronal magnetic field: latitudinally structured	uniform - no lat/lon dependence – consistent with observations (Smith & Balogh 1995, 2003; Acuña, 2008)
Predicts polarity, but strength in terms of total unsigned flux crossing SS	Can predict HMF strength & polarity